RSC Advances

ROYAL SOCIETY OF CHEMISTRY

www.rsc.org/advances

Journal Name

RSCPublishing

ARTICLE

Development of multifunctional biomimicking L-cysteine based oxovanadium(IV) complex: synthesis, DFT calculations, bromo-peroxidation and nuclease activity

Cite this: DOI: 10.1039/x0xx00000x

Received 00th January 2012,
Accepted 00th January 2012

DOI: 10.1039/x0xx00000x

www.rsc.org/

Urmila saha and Kalyan K. Mukherjea*

An oxovanadium complex [VO(sal-L-cys)(phen)] (sal-L-cys = Schiff base derived from salicylaldehyde and L-cysteine; phen = 1,10-phenanthroline) has been synthesized and characterized by spectroscopic studies (IR, UV-vis, ESI-MS and EPR studies) . The structure of the complex has been optimized by Density functional theory (DFT) calculations. Time-dependent DFT (B3LYP) calculations were used to establish and understand the nature of the electronic transitions observed in UV–vis spectra of the ligand and the complex. The multifunctionality of this oxovanadium complex has been exhibited by the application of it as catalyst in peroxidative bromination of phenol red to demonstrate vanadium dependent bromoperoxidase activity whereas nuclease activity has been established by DNA cleavage. The interaction of DNA with this structurally characterized oxovanadium complex has been studied by various physicochemical tools like UV-vis, fluorescence, viscosity measurement studies. The intrinsic binding constant of the complex with DNA has been determined determined by electronic absorption studies and calculated to be (3.51 ± 0.02) × 10^4 M^{-1}. The spectroscopic studies and the viscosity measurements indicate that the complex binds CT DNA by intercalative mode. The ability of the complex to induce DNA cleavage was studied by gel electrophoresis techniques. The complex has been found to promote cleavage of pUC19 plasmid DNA from the super coiled (SC) form I to nicked coiled (NC) relaxed form II.

Introduction

The continuous escalation of interest in the vanadium chemistry with multidented ligands is lying on the remarkable biological and pharmacological properties [1] of vanadium. Vanadium an essential biometal, is involved in various catalytic and inhibitory processes [2]. It is present in many abiotic as well as biotic systems. It also plays several roles such as cofactors in metalloenzymes [3] and metalloproteins [4]. Again, many oxovanadium complexes are known to possess potent insulin-mimetic effects [5] and anticancer activity [6], which deserves increasing application of vanadium complexes to biomedical sciences. The discovery of vanadium-dependent haloperoxidase enzymes (VHPO) in 1983 [7] from *Ascophyllum nodosum* marine algae boosts the attention of researchers to explore the coordination chemistry of vanadium for modeling various vanadium containing biomimetic and biomimicking molecules to get a better understanding on the mechanism of interaction of vanadium with the biogenic molecules. Vanadium haloperoxidase (VHPO) catalyses the oxidative halogenation of organic compounds [8] (hydrocarbons and alcohols, organic sulfide etc.) in presence of halide ions [9] and hydrogen peroxide under physiological conditions. Irrespective of their origin they all show a high degree of amino acid homology with oxovanadium moiety in their active centers. The peroxidative bromination is an important

route for the biosynthesis of many natural brominated organic compounds [10]. Such importance of the VPHO reactions warrants active research in developing newer and newer vanadium based complexes capable of mimicking VHPO activity. Moreover, development of metal based synthetic nucleases laid special attention in the chemotherapeutic research [11] since, they can be potentially used for cancer therapy or as restriction nucleases. Again, many oxovanadium complexes have been known to be the initiators in the photo-cleavage of DNA [12]. The transition metal complexes of 1, 10-phenanthroline or their modified variants have been widely employed [13] in DNA studies due to their applicability in bioinorganic and biomedicinal chemistry [14] as well as in the design of stereospecific DNA binding drugs [15]. Although, the synthesis of some oxovanadium complexes with various amino acid Schiff bases has been reported earlier [16], the detail investigation on the multifunctional activities i.e, the VPHO mimicking as well as nuclease activity by such complexes are scanty [17]. In the present work, synthesis, characterization, DFT calculations, catalytic activity and nuclease activity of an oxovanadium (IV) complex with the Schiff base derived from an amino acid (L-cysteine), and the 1,10 phenanthroline of the formula [$V^{IV}O$(sal-L-cys)(phen)] have been carried out with the aim of developing an amino acid based multifunctional biomimicking oxovanadium complex.

Experimental Section

Materials and Methods

All reagents and chemicals were procured commercially and of AR or GR grade (SD Fine Chemicals, India; and Aldrich) and used without further purification. Solvents were purified by standard procedures [18], wherever necessary. All solvents used for chromatographic analysis were either of HPLC, spectroscopic or GR grade and in all cases their purity was confirmed by GC analysis before use. Calf thymus DNA (CT-DNA) was purchased from the Sigma Chemical Company, USA; supercoiled (SC) plasmid pUC19 DNA was obtained from Bangalore Genei (Bangalore, India). The solutions of CT-DNA in phosphate buffer saline (PBS) medium [0.15 M, pH 7.2] gave a ratio of A_{260}/A_{280}, of ca. 1.8–1.85, indicating that the DNA was sufficiently free from protein contamination. The DNA concentration per nucleotide was determined by absorption spectrophotometry using the molar absorption coefficient (ε = 6600 M^{-1} cm^{-1}). Stock solutions were stored at 4 °C and used within 4 days.

Synthesis of the ligand (H_2sal-cys)

About 1.21 g (0.01 mol) of L-Cysteine and 1.22 g (0.01 mol) of salicylaldehyde were refluxed for 4 h in ethanol (50 mL). After cooling a pale yellow precipitate was formed, which was collected by filtration, washed with cold water and dried to give 2.24 g (92.18 %) of the schiff base. ^{1}H NMR (d, ppm; 300 MHz, DMSO-d_6): 3.13 (1H, s, -C$H_A$$H_B$SH), 3.17 (1H, s, -C$H_A$$H_B$SH), 3.40 (1H,s,-C<u>H</u>(N)(CH_2SH)), 5.57-5.64 (1H, m, Ar-C<u>H</u>=N-(geometrical isomers)), 6.93(4H,s,CH_2S<u>H</u>), 7.08–7.54 (4H,m) Ar-<u>H</u>, 8.42–8.64(1H, b,-COO<u>H</u>), 8.64(1H,b,-COO<u>H</u>), 10.31(1H,s,Ar-O<u>H</u>). ESI-MS(+ve) in MeOH: m/z (relative intensity) 226.05 [m^+ + 1], 248.03 [m^+ +23]. UV-vis in Methanol [λ_{max}nm (ε $M^{-1}cm^{-1}$)]: 323(8700), 279(12400), 255(27100), 218(36200). Elemental analysis: Calc. C 53.32 %, H 4.92 %, N 6.22 %; Found: C 53.40%, H 5.01 %, N 6.29 %.

Synthesis of the complex [$V^{IV}O$(sal-L-cys)(phen)]

A methanolic solution (10 ml) of the schiff base (H_2sal-cys) (0.01mol, 2.25g) was added to a 10 ml methanolic solution of vananadyl sulfate pentahydrate (0.01 mol, 2.53 g) with continuous stirring, followed by dropwise addition of a methanolic solution (5 ml) of 1,10-phenanthroline monohydrate (0.01 mol,1.98 g) and stirred for another 2 h, which on standing produced brown yellow solid (Scheme 1). The brown yellow solid was collected by filltration, washed with cold water and dried under vaccum. Yield: 77%. IR (KBr, cm^{-1}): 3419.96 [υ(O-H)], 2612.79 [υ(S-H)], 1601.93 [υ_{as}(COO)], 1645.27 [υ(C=N)], 968.37 [υ(V=O)]. ESI-MS(+ve) in MeOH: m/z (relative intensity) 471.11 [m^+ + 1], 493.08 [m^+ + 23]. UV-vis in Methanol [λ_{max}nm (ε $M^{-1}cm^{-1}$)]: 382(4760), 264(33000), 218 (49200). Elemental analysis: Calc. C 56.17%, H 3.64%, N 8.93 %; Found: C 56.31%, H 3.61 %, N 8.89 %.

Physical measurements

The IR spectra were taken as KBr discs at room temperature on a Perkin Elmer RFX-I IR spectrophotometer. Elemental analyses were carried out using a Perkin–Elmer 2400 series II CHNS analyzer. UV-vis spectra (200–800 nm) were recorded against appropriate reagent blank at room temperature with a Schimadzu U-1200 spectrophotometer using 1cm quartz cell. EPR spectra were obtained on a JEOL – JES FA200 ESR spectrometer in DCM – toluene (1:1) glass at 77K. NMR spectral measurements were carried out in DMSO-d_6 solution at ambient temperature. The ^{1}H NMR spectra were taken by Bruker 300 MHz NMR spectrometer and the mass spectral analyses were done in methanol solvent from Waters mass spectrometer (model: XEVO-G2QTOF#YCA351). The gel electrophoresis study was carried out with UVP Bio Doc-It Imaging System and nicking was analysed by UVP DOC-ItLS software.

Journal Name

RSCPublishing

ARTICLE

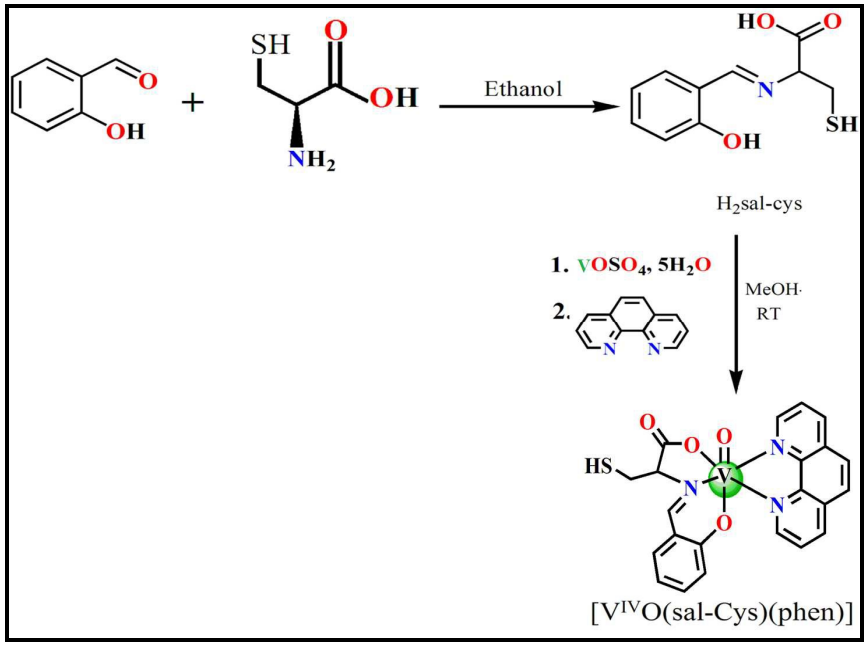

Scheme 1. Synthesis of [VO(sal-L-cys)(phen)]

DFT calculations

DFT study is an important tool which provides understanding on the geometry, electronic structure, and optical properties of the system in question. Ground state electronic structure calculations in methanol solution of both the ligand and the complex have been carried out using DFT [19] method associated with the conductor-like polarizable continuum model (CPCM) [20]. Becke's hybrid function [21] with the Lee-Yang-Parr (LYP) correlation function [22] was used in the study. The geometry of the ligand and complex was fully optimized without any symmetry constraints. On the basis of the optimized ground state geometry, the absorption spectral properties in methanol (CH_3OH) media were calculated by time-dependent density functional theory (TDDFT) [23] approach associated with the conductor-like polarizable continuum model (CPCM) [20]. We computed the lowest 40 singlet – singlet transitions and results of the TD calculations were qualitatively very similar. The TDDFT approach has been demonstrated to be reliable for calculating spectral properties of many transition metal complexes [24]. Due to the presence of electronic correlation in the TDDFT (B3LYP) method it can yield more accurate electronic excitation energies. Hence, TDDFT had been shown to provide a reasonable spectral feature for our complex of investigation.

For H atoms we used 6-31G basis set; for C, N, O and V atoms basis set was employed 6-31G and for S atom we adopted 6-31 + G(d,p) as basis set for the optimization of the ground state. The calculated electronic density plots for frontier molecular orbitals were prepared by using Gauss View 5.1 software. All the calculations were performed with the Gaussian 09W software package [23]. Gauss Sum 2.1 program [25] was used to calculate the molecular orbital contributions from groups or atoms.

Bromination of alkenols using the complex as catalyst

Halogenation was carried out by the catalytic bromination of phenol red to bromophenol blue using the oxovanadium complex as a catalyst. The catalytic activity of the complex was studied by absorption spectroscopy. Bromination reaction activity tests were carried out at a constant temperature of (30±0.5) ° C in presence of H_2O_2 and KBr in mild acidic medium. An aliquot of 30% H_2O_2(final concentration 2.0 mM) was added to a H_2O-DMF solution (with a volume ratio of 4:1) of catalyst followed by the addition of 4.0 mol/L of KBr.

Solutions used for kinetic measurements were maintained at pH=5.8 by the addition of NaH_2PO_4- Na_2HPO_4 [26]. Reactions were initiated by the addition of 0.1 mmol of phenol red. Bromination of phenol red was monitored by the measurement of the increase in the absorbance at 592 nm for reaction at specific time points. The spectral data show the gradual disappearance of the peak at 443 nm due to the loss of phenol red and an increase in the absorbance of the peak at 592 nm due to the formation of the bromophenol blue product and spectral changes were recorded at the intervals of 5 min.

The rate of this reaction is described by the rate equation: $dc/dt = kc_1^x c_2^y c_3^z$, from which the equation "$\log(dc/dt) = \log k + x \log c_1 + y \log c_2 + z \log c_3$" was obtained, corresponding to "$-\log(dc/dt) = -x \log c_1 - b$ ($b = \log k + y \log c_2 + z \log c_3$)", where k is the reaction rate constant; c_1, c_2, c_3 are the concentrations of the oxovanadium complex, KBr and phenol red,respectively; while x, y, z are the corresponding reaction orders. According to Lambert–Beer's law, $A = \varepsilon dc$, which on differentiation we get $dA/dt = \varepsilon d(dc/dt)$, where '$A$' is the resultant absorbance; 'ε' is the molar absorption coefficient (for bromophenol blue ε = 14 500 M^{-1} cm^{-1} at 592 nm); 'd' is the light path length of the sample cell (d = 1). The absorbance data were plotted against the reaction time, a straight line was obtained and the reaction rate (dA/dt) was obtained from the slope of this line. The reaction rate constant (k) can be obtained from the plot of $-\log(dc/dt)$ *versus* $-\log c_1$. In the experiment, the reaction orders of KBr and phenol red (y and z) were taken as 1 according to the literature [27], c_2 and c_3 are known as 0.4 and 10^{-4} mol L^{-1}, respectively.

DNA binding studies and nuclease activity

UV–vis spectral study

UV–vis spectra were recorded in a Schimadzu U-1200 spectrophotometer using Quartz cuvettes of 1cm path length. The electronic absorption spectra were monitored in PBS (0.15M, pH 7.2) buffer at room temperature 25^0 C by keeping the concentration of the CT-DNA constant (10 µM), while varying amounts of complex [in 1 % methanol- PBS buffer (v/v) solution] over a range of 1–12 µM. While measuring the absorption spectra, equal amounts of complex was added to both the test and the reference solutions to eliminate any absorbance of the complex itself.

Fluorescence study

Competitive ethidium bromide (EB) binding experiment was carried out to investigate the binding mode of the complex to CT-DNA. The fluorescence was measured by a Perkin Elmer LS55 spectrofluorimeter. The experiment was monitored by the addition of 10.0 µM of CT-DNA in Tris–HCl/NaCl buffer to a 15 µM solution of ethidium bromide in the same buffer medium. Aliquot of stock solution of the complex [1% MeOH–buffer (v/v) solution] was added to the ethidium bromide bound CT-DNA solution in a way so that, the ratio of [complex] / [EB-DNA] were 0, 0.2, 0.4, 0.6, 0.8, 1.0, 1.2 and the respective solutions were incubated for 2 h at 37°C, thereafter, the fluorescence intensities of the solutions were recorded by exciting the solutions at 500nm whereas slits for both the excitation and emission were 10 nm.

Viscometric study

The viscosity of sonicated DNA (average molecular weight of ~200 base pairs obtained using a Labsonic 2000 sonicator) [28] was measured by a fabricated micro-viscometer maintained at 28 (± 0.5) °C in a thermostatic water bath. Data were presented as $(\eta/\eta_o)^{1/3}$ vs the ratio of the concentration of metal complex to that of the CT-DNA, where η and η_o are the viscosities of the CT-DNA solutions in the presence and absence of the complex, respectively. The viscosity of DNA ($\eta = t - t_o$) was calculated from the observed flow time of CT-DNA solutions (t) and buffer solution (t_o).

Gel electrophoresis study

DNA cleavage activity of the complex was monitored with the help of a Gel electrophoresis Model No. 2101, Genei, Bangalore. The super coiled pUC19 DNA (0.5 µg per reaction) in Tris-HCl/NaCl buffer (pH 7.2) was treated with increasing amounts of metal complex over a range of 20–60 µM alongwith H_2O_2 (4 µM) [29]. After incubation for 2 h at 37 °C, it was mixed with a sample loading dye. The samples were run on a 0.9% agarose in 1X TAE buffer for 3 h at 80 mV, then it was treated with EB solution and the bands were visualized by UV light and photographed with UVP Bio Doc-It Imaging System. The percentage of cleavage of super coiled (SC) pUC19 DNA cleavage induced by the complex was determined by using UVP BIODOC-ItLS software.

Results and discussion

IR and UV–vis spectrophotometric characterization of the complex

The characteristic $\upsilon_{(V=O)}$ vibration [9, 11] of oxovanadium (IV) complex appears at 968.37 cm^{-1} as a sharp band. The complex presents very strong bands at 1645.27 cm^{-1} and 1601.93 cm^{-1}; these correspond to $\upsilon_{(C=N)}$ and $\upsilon_{as(COO)}$ respectively of the Schiff base ligand. The strong vibrations at 1438.25 cm^{-1} and at 736.03 cm^{-1} are due to the $\upsilon_{(C-N)}$ vibration of the phen ligand in the complex, which apprared at 1421 cm^{-1} and 731 cm^{-1} respectively in the uncoordinated phenanthroline. The electronic absorption bands of the oxovanadium(IV) complex in methanol solution at the 382nm, 218nm and 264 nm are assigned as intra ligand charge transfer transitions [30].

Mass spectrometric analysis

The molecular formulation and some structural information can be obtained from ES-MS analysis and elemental analysis. The molecular formula of the complex [VO(Sal-Cys)(Phen)] obtained from elemental analysis is supported by the

observation of peak at m/z (relative intensity): 471.11 [m^+ + 1], 493.08 [m^+ + 23].

Geometry optimization and electronic structure determination by DFT calculation

The optimized geometry of the ligand (H_2sal-cys) and its oxo vanadium complex is shown in Fig.1a and Fig.1b respectively. For both the ligand and the complex, only the ground state geometries have been optimized. Main optimized geometrical parameters of the oxovanadium complex are listed in Table 1. The hexa-coordinated metal centre possesses a distorted octahedral geometry in the complex. All calculated V-N distances occur in the range 2.073-2.419 Å and V-O distances are in the range 1.614-1.979 Å whereas, on complexation, some C-N and C-O bond lengths are changed with respect to that in free ligand and Table 2 describes the change in bond lengths in the complex compared to the free ligand (H_2sal-cys).

Table 1 Selected optimized geometrical parameters for the oxovanadium complex in the ground state calculated at B3LYP Levels.

Bond Lengths (Å)			
V-N1	2.073	V-O1	1.958
V-N2	2.173	V-O2	1.979
V-N3	2.419	V-O3	1.614
Bond Angles (°)			
N1-V-N3	93.626	N2-V-O2	91.910
N2-V-N3	71.902	N2-V-O3	91.200
N2-V-Ol	95.616	N1-V-O1	87.290
O1-V-N3	79.136	N1-V-O2	78.772
O3-V-N3	163.102	N1-V-N2	161.950
O1-V-O2	152.050	O2-V-O3	103.007

Table 2 Change in bond lengths for the oxovanadium compared to free the ligand (H_2sal-cys) in the ground state calculated at B3LYP Levels

Bond Lengths (Å)		
	Ligand (H_2sal-cys)	Oxovanadium complex
O1-C1	1.362	1.290
N1-C3	1.303	1.302
N1-C4	1.486	1.472
O2-C5	1.369	1.291

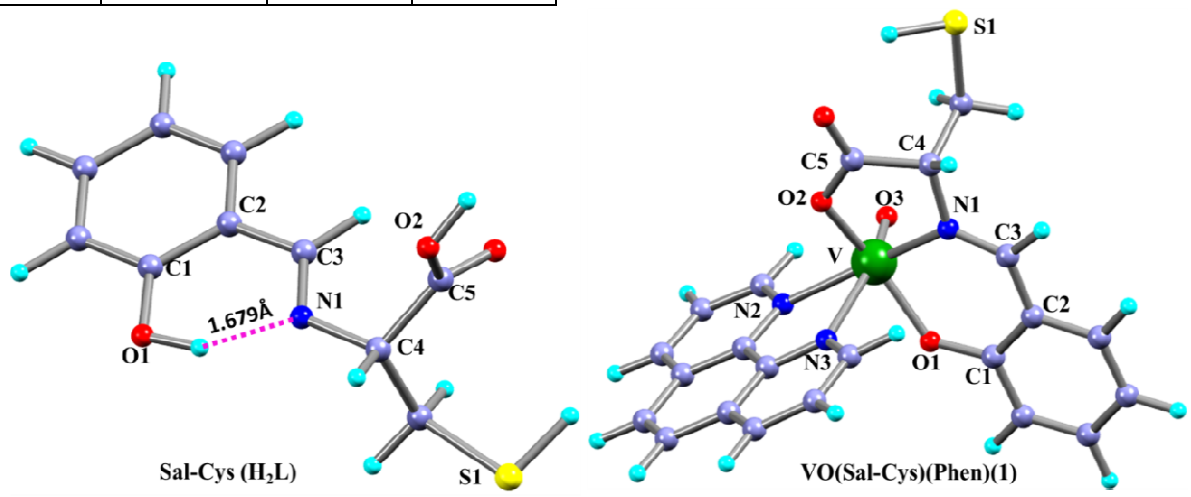

(a) **(b)**

Fig. 1 Optimized geometry of the free ligand (H_2Sal-Cys) and the Complex [VO(Sal-Cys)(Phen)] under DFT[B_3LYP (6-31G)].

Journal Name RSCPublishing

ARTICLE

In case of the free ligand (H_2Sal-Cys) at the ground state, the electron density at HOMO and LUMO+2 orbitals mainly reside on the salicylaldehyde moiety while a considerable contribution comes from cysteine moiety along with the contribution of salicylaldehyde moiety in HOMO–2, HOMO–1, LUMO and LUMO+1 orbitals. The energy difference (Fig. 2) between HOMO and LUMO is 4.328 eV of the ligand (H_2Sal-Cys). In case of the oxovanadium complex all the HOMO-3, HOMO -2 and HOMO orbitals are mainly originating from salicylaldehyde-cysteine π and π* orbital contribution while the LUMO, LUMO +1 and LUMO +3 orbitals arise from metal d orbital contribution along with the π orbital contribution of 1,10- phenanthroline. The energy difference between HOMO and LUMO is 3.068 eV of the complex (Fig. 2).These compositions are useful in understanding the nature of transition as well as the absorption spectra of both the ligand and the complex (*vide infra*).

The ligand shows four absorption bands at 323, 279, 255 and 218 nm in methanolic solution at room temperature. These four absorption bands can be assigned to the $S_0 \rightarrow S_1$, $S_0 \rightarrow S_4$, $S_0 \rightarrow S_7$ and $S_0 \rightarrow S_{10}$ transitions (Fig. 3) from TDDFT calculations. The absorption energies along with their oscillator strengths, the main configurations and their assignments calculated using TDDFT method for the ground state geometry for H_2L is discussed here and the related data are given in Table 3.

The complex shows three absorption bands at 382, 264 and 227 nm in methanolic solution at room temperature. The calculated absorption bands are located at 385 and 259 nm in the complex (Fig. 4), which are in good agreement with the experimental results of 382 and 264nm (Table 4). These two absorption bands can be assigned to the $S_0 \rightarrow S_{18}$ and $S_0 \rightarrow S_{24}$ transitions, respectively (Table 4).

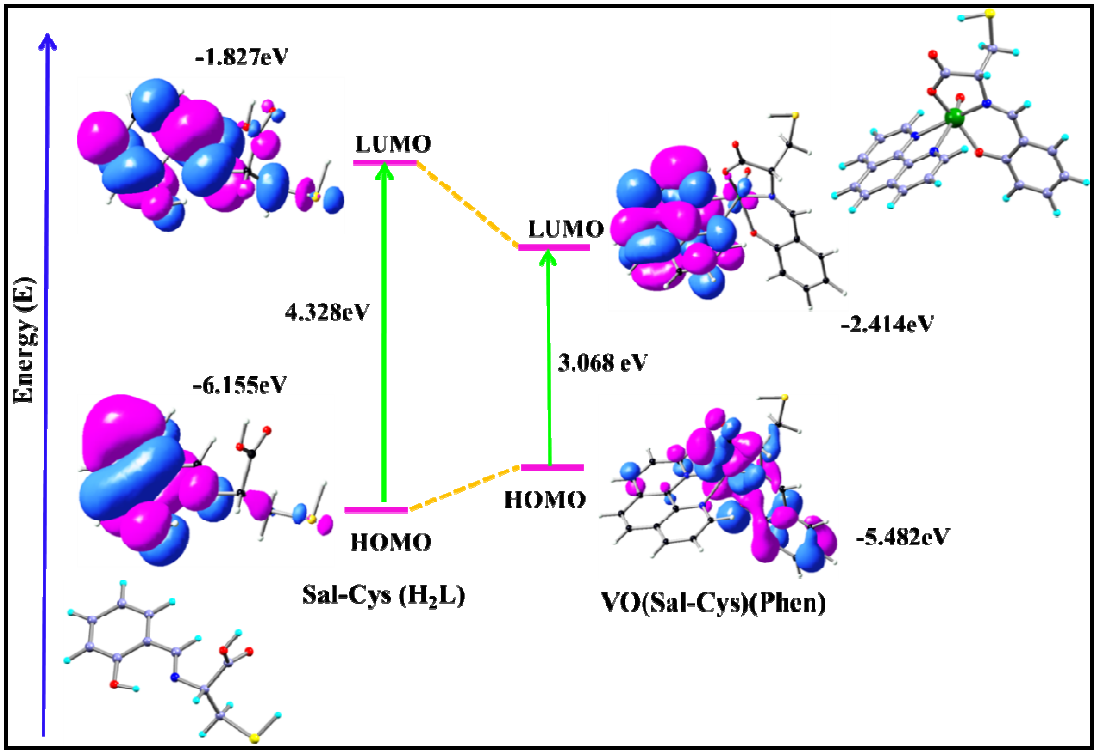

Fig.2 Frontier molecular orbital of complex as well as ligand optimized under [B3LYP (6-31G)].

Journal Name RSCPublishing

ARTICLE

Table 3 Selected Parameters for the vertical excitation (UV-vis absorptions) of the free ligand (H_2Sal-Cys); electronic excitation energies (eV) and oscillator strengths (*f*), configurations of the low-lying excited states of the ligand; calculations of the $S_0 \rightarrow S_n$ energy gaps are based on optimized ground-state geometries (UV-vis absorption) (CH_3OH used as solvent).

Electronic transition	Composition	Excitation energy	Oscillator strength (*f*)	CI	λ_{exp} (nm)
$S_0 \rightarrow S_1$	HOMO–2 → LUMO HOMO–1 → LUMO HOMO→ LUMO	3.7738 eV (328nm)	0.0617	0.21195 0.50636 -0.42029	323
$S_0 \rightarrow S_4$	HOMO–3→ LUMO HOMO–3→ LUMO + 1 HOMO–2→ LUMO + 1 HOMO–1→ LUMO	4.3852 eV (282 nm)	0.0510	0.26802 0.10157 0.21231 0.25215	279 255
$S_0 \rightarrow S_7$	HOMO–3→ LUMO +1 HOMO–1→ LUMO + 1 HOMO–2→ LUMO	4.9183 eV (252 nm)	0.1337	0.27380 0.26486 -0.18159	 218
$S_0 \rightarrow S_{10}$	HOMO–1→ LUMO +2 HOMO→ LUMO +2	5.7118 eV (217 nm)	0.0851	0.49863 -0.41682	

Table 4 Simulated values of various factors of the optical transitions for the oxovanadium complex.

Electronic transition	Composition	Excitation energy	Oscillator strength (*f*)	CI	λ_{exp} (nm)
$S_0 \rightarrow S_{18}$	HOMO – 2 → LUMO HOMO – 2 → LUMO+3 HOMO → LUMO + 3	3.2192 eV (385 nm)	0.0891	0.23713 0.15239 -0.17791	382
$S_0 \rightarrow S_{24}$	HOMO – 3→ LUMO + 1 HOMO – 2→ LUMO	4.2856 eV (259 nm)	0.1257	0.26945 0.39122	264

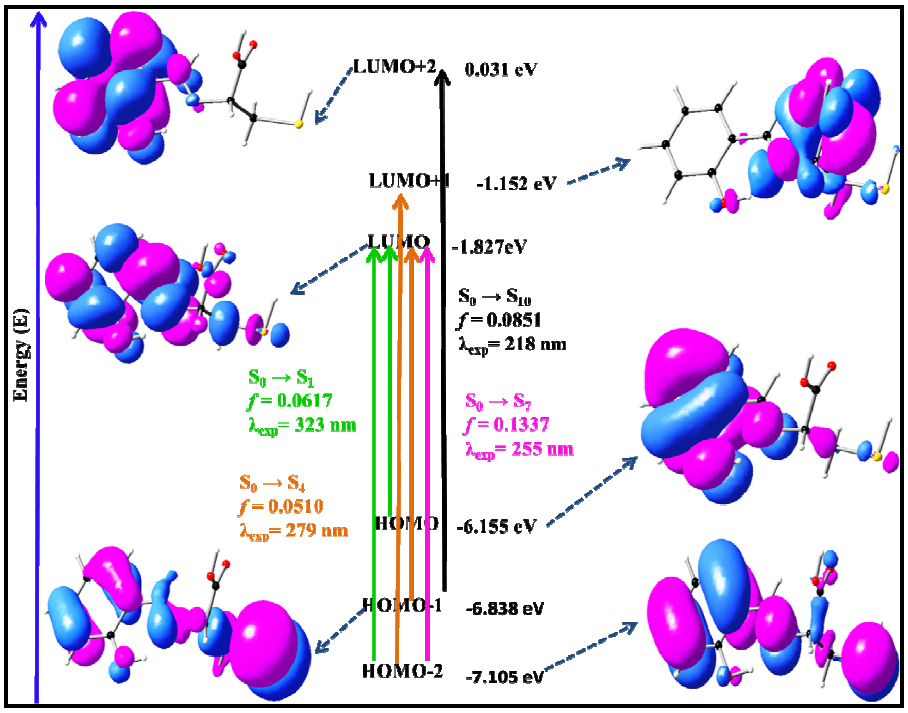

Fig. 3 Frontier molecular orbitals involved in the UV-vis absorption of the free ligand (H_2Sal-Cys).

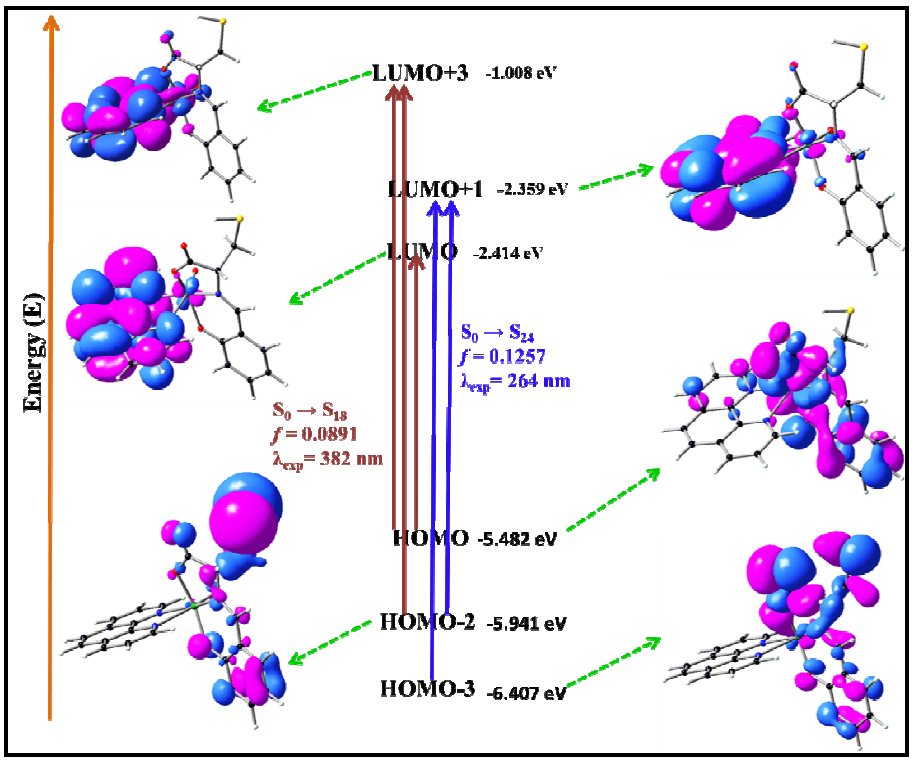

Fig. 4 Frontier molecular orbitals involved in the UV-vis absorption of the oxovanadium complex.

EPR study

EPR spectroscopy is a powerful tool that provides information about the nuclearity (Fig.5), and electronic structure of a paramagnetic state. X-band EPR spectra of the complex [$V^{IV}O$(sal-L-cys)(phen)] was recorded in frozen (77K) dichloromethane – toluene (1:1) glass. It gives rise to well resolved ^{51}V (I = 7/2) hyperfine eight lines and the spectral parameters are listed in table 5. The spectrum has axial symmetry with $g_{\|} < g_{\perp}$. The caracteristic $g_{\|} < g_{\perp}$ and $a_{\|} >> a_{\perp}$ relationship corresponding to an axially compressed d^1xy configuration [31, 32] was observed. The EPR study confirms the presence of mononuclear vanadium(IV) moiety in the complex.

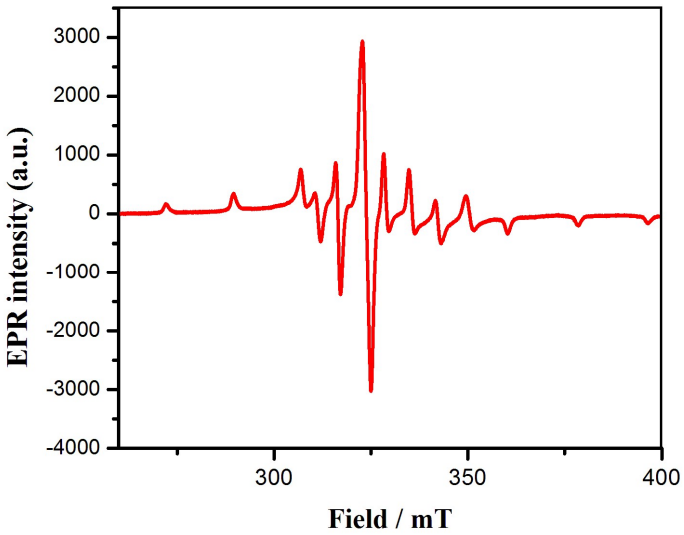

Fig.5 EPR spectrum of complex in solution (DCM / toluene) at 77K.

Table 5 EPR spectral data at 77K in solution DCM – toluene (1:1)

Compound	$g_{\|}$ ($A^{\|}$ / G)	$g^{\perp}$ ($A^{\perp}$ /G)	gav (A_{av} /G)
[$V^{IV}O$(sal-cys)(phen)]	1.948 (71.88)	1.987 (57.25)	1.974 (61.24)

Therefore, all the above spectroscopic findings along with DFT calculations suggest that the molecular geometry of the complex is [$V^{IV}O$(sal-L-cys)(phen)] with O, N, O linkage from the schiff base, N,N coordination from o-phenanthroline and the oxo linkage.

Biomimicking catalysis by the compound

Many oxovanadium complexes are found to mimic the vanadium haloperoxidases catalyzes the bromination of organic substrates in the presence of H_2O_2 and bromide. The catalytic haloperoxidase activity of vanadium complexes is often investigated by the kinetic study of the catalytic bromination of phenol red to bromophenol blue as a model system. The catalytic ability of the oxovanadium complex [$V^{IV}O$(sal-L-cys)(phen)] for the oxidative bromination of phenol red was monitored by UV–vis spectrophotometry (Fig. 6). The gradual decrease in the absorbtion at 443 nm due to disappearance of phenol red and the appearance of a new peak at 590 nm due to formation of bromophenol indicate the conversion of phenol red to bromophenol blue, and the reaction was complete after ~8 h under ambient conditions. The plots for the kinetic studies of the above conversion are shown in Fig. 7 and Fig. 8. The same reaction was monitored without addition of the oxovanadium complex whereby no appreciable change could be observed.

Mechanism of the catalytic activity

The mechanism of catalytic activity is assumed to be similar as decribed in our previous work [11]. During the catalytic process, the catalyst (I) was converted to a bound peroxide intermediate (III) in presence of peroxide in mild acidic medium. This intermediate in turn oxidizes the bromide (Br^-) ion in the medium to bromonium ion (Br^+) which exists in reaction medium as Br_3^-, Br_2 or HOBr [8]. Attack of a bromide ion at one of the peroxo atoms (IV) and the uptake of a proton from a surrounding water molecule leads to the generation of hypobromous acid (HOBr) (V) followed by restoration of the native state (I). The in situ generated bromonium ion reacts with the organic substrate (phenol red) to form corresponding brominated derivatives. The catalytic cycle has been depicted in scheme-2.

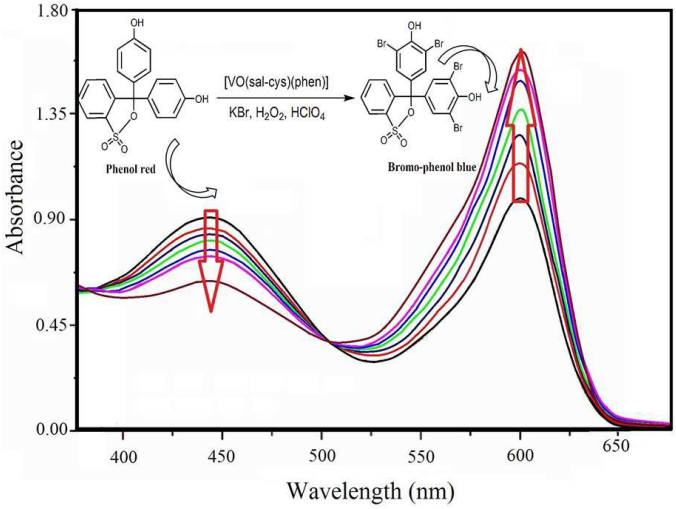

Fig.6 Oxidative bromination of phenol red catalyzed by the oxovanadium complex (0.04 mmol). Spectral changes at 10 min intervals. Spectral data taken of aliquots in pH = 5.8 aqueous phosphate buffer, c(phosphate buffer) = 50 mmol L^{-1}, c(KBr) = 0.4 mol L^{-1}, c(phenol red) = 10^{-4} mol L^{-1}.

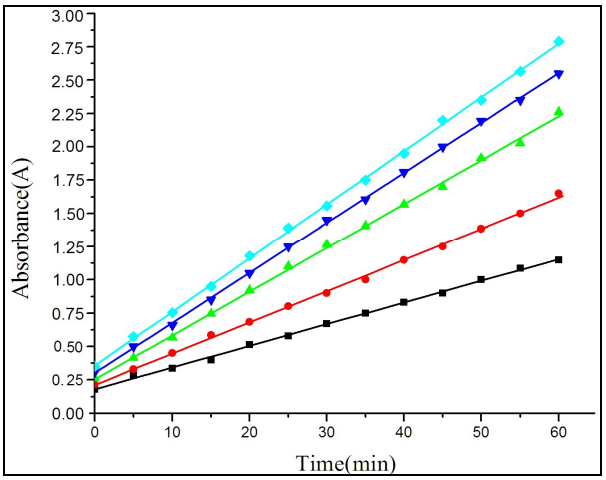

Fig.7 The measurable absorbance dependence on time for the oxovanadium complex.Conditions used: pH = 5.8, c(KBr) = 0.4 mol L^{-1}, c(H_2O_2) = 2 mmol L^{-1}, c(phenol red) = 10^{-4} mol L^{-1}. c(complex/mmol L^{-1}) = a: 2×10^{-2}; b: 4×10^{-2};c: 6×10^{-2}; d: 8×10^{-2}; e: 1×10^{-1}.

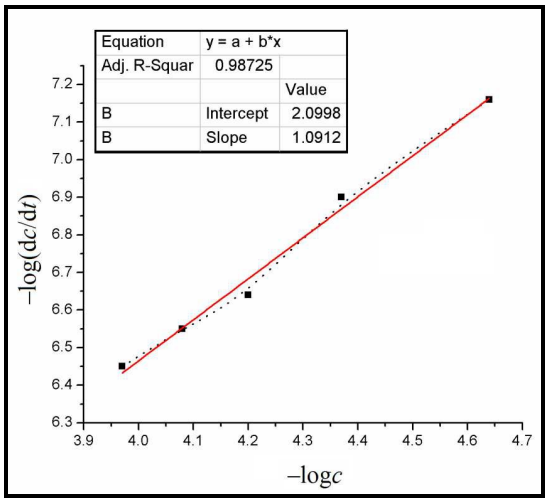

Fig.8 -log(d*c*/d*t*) dependence of -log*c* (*c* is the concentration of the oxovanadium complex; conditions used: c(phosphate buffer) = 50 mmol L^{-1}, pH = 5.8, c(KBr) = 0.4 mol L^{-1}, c(phenol red) = 10^{-4} mol L^{-1}.

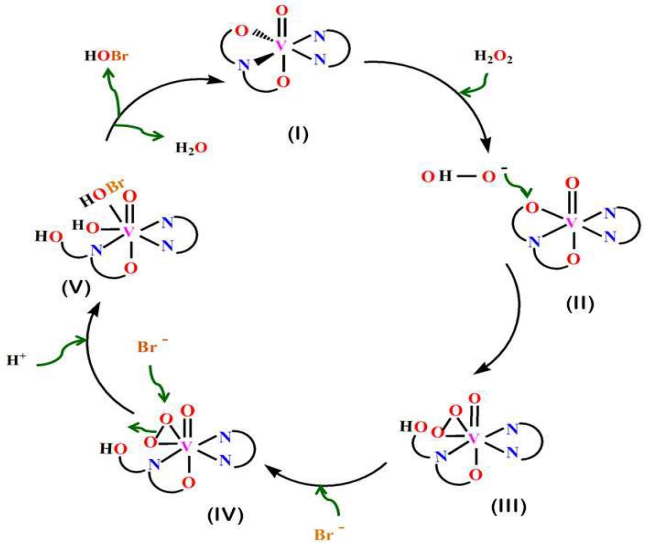

Scheme 2 Schematic representation of the proposed mechanism of the catalytic bromination of the complex [V^{IV}O(sal-cys)(phen)] as a catalyst in presence of KBr and H_2O_2 in acidic medium.

Nuclease activity of the oxovanadium complex

Spectrophotometric studies on DNA binding by the complex

Electronic absorption spectroscopy is usually used to determine the binding of metal complexes with DNA. A complex bound to DNA through intercalation is characterized by the change in absorbance (hypochromism) and red shift in wavelength, due to the stacking interaction between the aromatic chromophore and the DNA base pair [33, 34, 35]. To

calculate the complex-DNA binding constant (K_b),the data are treated according to the following equations [33]:

$$1/(A-A_0) = 1/(A_\infty-A_0) + 1/K(A_\infty-A_0) \cdot 1/C_{ligand}$$

Where, A_o is the absorbance of DNA at 260 nm in the absence of complex, A_∞ is the final absorbance of the ligated DNA, and A is the recorded absorbance at different ligand concentrations. The absorption spectrum of CT-DNA at 260 nm is monitered by varying the concentration of the oxovanadium complex. Upon the addition of incremental amounts of complex hypochromism was observed **(Fig.9)** without any significant red or blue shift. The double reciprocal plot of $1/(A-A_o)$ versus $1/C_{ligand}$ is linear, and the binding constant (K) can be estimated from the ratio of the intercept to the slope **(Fig.10)**. The complex shows binding constant as $(3.51 \pm 0.02) \times 10^4$.

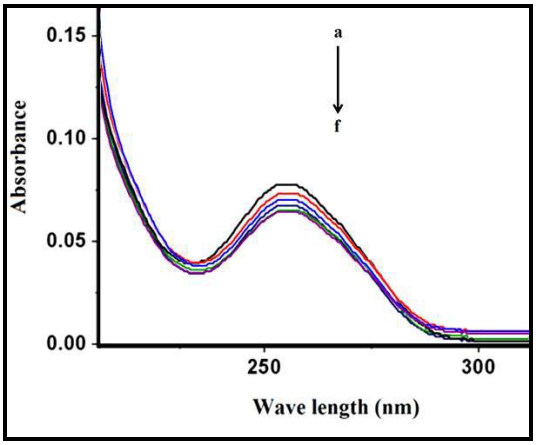

Fig. 9 Absorption spectra of DNA upon increasing amounts of complex, [Complex]/[DNA] = 0.2; 0.4; 0.6; 0.8; 1.0; 1.2.

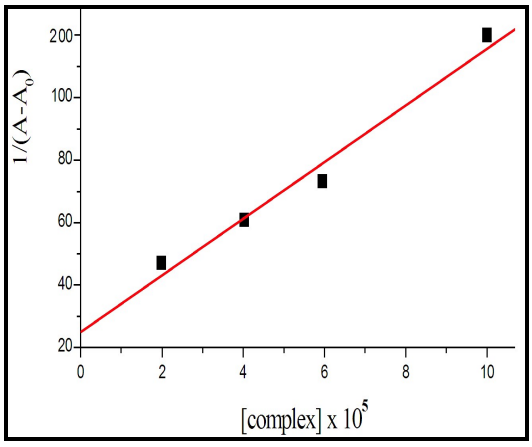

Fig. 10 Plot of $1/(A-A_o)$ *versus* [complex] $\times 10^5$ (M^{-1})

Fluorescence emission titrations for DNA interaction

Fluorimetric measurements using ethidium bromide (EB) as a probe are usually carried out to establish the binding mode of small molecule to the double-helical DNA. Ethidium bromide(EB) emits intense fluorescence in the presence of DNA due to its strong intercalation between the adjacent DNA base pairs. This enhanced fluorescence can be quenched by the addition of a third molecule which can bind DNA by intercalative mode by displacing EB [29, 36, 37]. The emission spectra of EB bound to DNA in the absence and presence of the complex are presented in Fig. 11. The addition of the complex to DNA pretreated with EB causes a gradual quenching in emission intensity, indicating that the complex competes with EB in binding DNA, which leads to a quenching in the fluorescence intensity of EB-DNA complex system. In fact, as expected for a displacement effect, the increase in the concentration of complex gradually quenches the fluorescence intensity of EB-DNA complex system. This significant decrease in fluorescence intensity lends strong support in favor of intercalation of the complex into the DNA double helix by displacing EB. Fluorescence quenching study in presence of the complex was analyzed further by Stern-Volmer equation: $I_0/I = 1 + K_{SV}[Q]$ [29]; where I_0 and I are the fluorescence intensities in absence and presence of quencher (complex) respectively; [Q] is the concentration of the quencher, K_{SV} is the Stern-Volmer quenching constant, which is obtained from the slope of plot of I_0/I vs. [Q]. A plot of I_0/I vs. [complex]/[DNA] appears linear (Fig. 12) and the Stern-Volmer quenching constant (K_{SV}) was found to be $(5.24 \pm 0.02) \times 10^4 M^{-1}$ at 37 ºC. This data is also in agreement with the value obtained by electronic spectral studies [29, 36, 37].

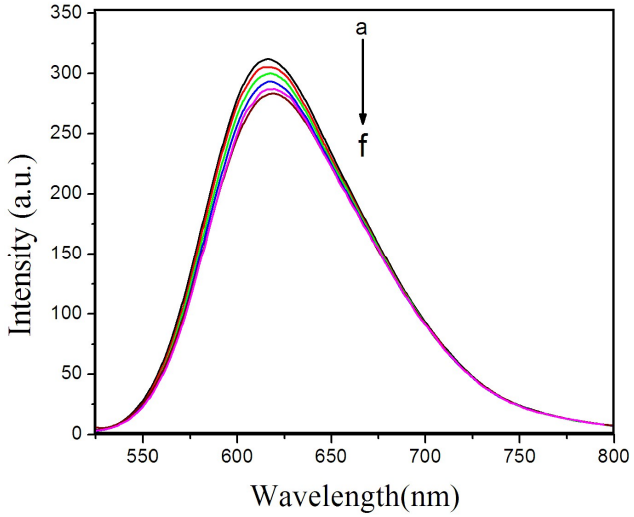

Fig. 11 Fluorescence emission spectra of the EB-DNA complex in the presence of [EB] = 15 µM + [DNA] = 10.0 µM; the ratio of [VO(sal-cys)(phen)] / EB-DNA = 0, 0.2, 0.4, 0.6, 0.8, 1.0, 1.2. Excitation wave length=500 nm.

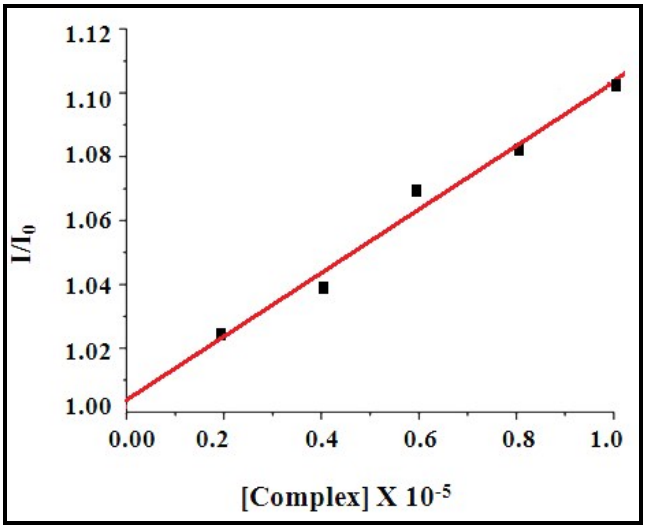

Fig. 12 Plot of I/I_0 vs. [VO(sal-cys)(phen)] / DNA

Viscometric studies to confirm the DNA binding pattern

Viscometric studies play a very important role in ascertaining DNA binding pattern in solution. More precisely, it can lend strong support in favour of intercalative binding. The intercalative binding by the ligand lengthens the DNA helix, which in turn, causes an increase in the viscosity of DNA [38]. The values of relative specific viscosities of DNA in the absence and presence of the complex are plotted against [complex] / [DNA] and are presented in Fig.13. It is observed that the addition of the complex to the CT-DNA solution leads to an increase in the viscosity of the CT-DNA, thereby clearly demonstrating the intercalative binding of the complex to CT-DNA [38, 39].

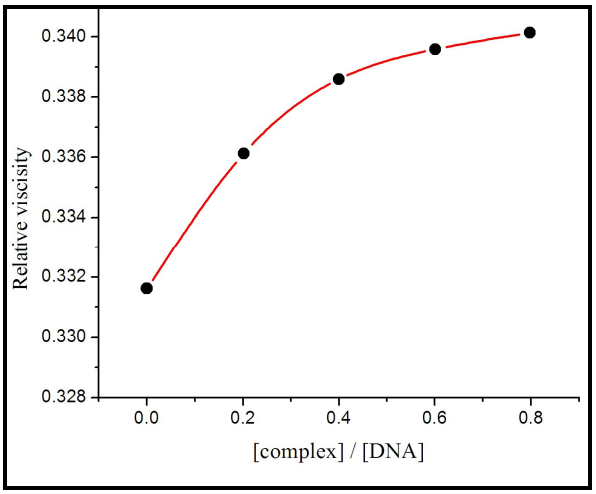

Fig. 13 Effect of increasing amount of [VO(sal-cys)(phen)] complex on the specific viscosity of CT DNA. Samples were prepared so as to give total complex/base pair ratios of 0, 0.2, 0.4, 0.6, and 0.8.

Gel electrophoresis study for nuclease activity

The double-stranded plasmid pUC19 DNA exists in a compact supercoiled (SC) form. Upon introduction of strand breaks, the supercoiled form of DNA is disrupted into the nicked circular (NC) form or the linear form. If one strand is cleaved, the super coiled form will relax to produce a nicked circular form. If both the strands are cleaved, a linear form will be produced. Relatively fast migration is observed for super coiled form when the plasmid DNA is subjected to electrophoresis, while the nicked circular form migrates slowly and the linear form migrates in between SC and NC [9, 29, 37]. Hence, DNA strand breaks could be quantified by measuring the transformation of the super coiled form into nicked circular and linear forms. The ability of the vanadium complex to induce DNA cleavage was studied by gel electrophoresis using super coiled pUC19 DNA in Tris-HCl/NaCl buffer (pH 7.2). The results of the Gel electrophoresis (Fig. 14) experiment and quantitative cleavage data are presented in Table 6. In the gel electrophoresis six bands are observed. Lane 1 contains only DNA and has 87% supercoiled form i.e., Form I and 13 % relaxed form i.e., Form II. On the addition of H_20_2 (4 µM), percentage of relaxed form increases to 28 % (Lane 2) while on addition of the compound (20 µM to 60 µM), the percentage of relaxed form increases through 31 to 39 to 51 in lane 3, 5, 7 respectively. Whereas, on addition of different concentrations of compound and H_20_2 together (4 µM H_20_2+ 20 µM), (4 µM H_20_2+ 40 µM) and (4 µM H_20_2+ 60 µM) the percentage of relaxed form of DNA increases to 36 % (lane 4), 45 % (lane 6) and 69 % (lane 8) respectively. This clearly indicates that the compound alone shows moderate nuclease activity but exhibits greater nuclease activity at higher concentration when used in combination with H_20_2 [9, 29, 37].

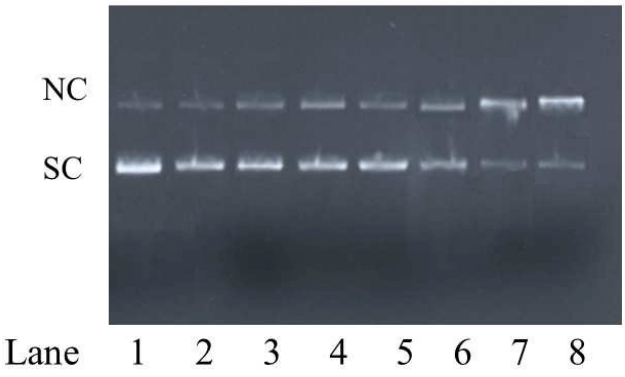

Fig. 14 (a) Agarose gel(0.9 %) electrophoregram of supercoiled DNA (0.5 µg) incubated for 45 min at 37 °C, in PBS buffer (0.15 M, pH 7.2) at 37 °C. Lane 1: DNA control; Lane 2: DNA+ H_2O_2; Lane 3: DNA + complex (20 µM); Lane 4: DNA+ complex

(20 μM) + H_2O_2; lane 5: DNA + complex (40 μM); lane 6: DNA+ complex (40 μM) + H_2O_2; lane 7: DNA + complex (60 μM); lane 8: DNA+ complex (60 μM) + H_2O_2

Table 6. Results of the cleavage of pUC19 DNA determined by gel electrophoresis study

Sl No.	Reaction condition	Form I (% SC)	Form II (%NC)
Lane 1	control DNA	87	13
Lane 2	DNA + H_2O_2 (4 μM)	72	28
Lane 3	DNA+ complex (20 μM)	69	31
Lane 4	DNA+ complex (20 μM)+ H_2O_2	64	36
Lane 5	DNA + complex (40 μM)	61	39
Lane 6	DNA + complex (40 μM) + H_2O_2	55	45
Lane 3	DNA+ complex (60 μM)	49	51
Lane 6	DNA + complex (60 μM) + H_2O_2	31	69

Conclusion

A new oxovanadium complex [$V^{IV}O$(sal-cys)(phen)] has been designed and synthesized with the aim of developing multifunctional molecule, active both in the fields of biocatalysis as well as in DNA knicking . The compound mimics the in vitro bromination of organic substate giving corresponding brominated product. The results of physicochemical studies of DNA binding as well as DNA cleavage activity indicate that the oxovanadium(IV) compound may be useful in DNA manipulation studies. Hence, the newly synthesized complex [$V^{IV}O$(sal-cys)(phen)], exhibits versatile multifunctional enzyme mimetic catalytic activities both as a bromoperoxidase as well as a DNA nuclease.

Acknowledgements

The authors are thankful to UGC, New Delhi for financial support in the form of a Major Research Project [Sanction no.39-706/2010(SR)] to K.K.M., where U.S. had been a project fellow..

Notes and references

Department of Chemistry, Jadavpur University, Calcutta (Kolkata), 700032, India. ∗Corresponding author. Tel.: +91 9831129321; fax: +91 33 24146223.E-mail address: k_mukherjea@yahoo.com (K.K. Mukherjea).

†Electronic Supplementary Information (ESI) available: [details of any supplementary information available should be included here]. See DOI: 10.1039/b000000x/.

References

1 (a) D. Rehder, *Future Med. Chem.*, 2012, **4**, 1823–1837; (b) H. Vilter, *Metal Ions in Biological Systems: Vanadium and its Role in Life*, H. Sigel, A. Sigel, Eds. Marcel Dekker: New York, 1995, **31**, Chapter 10, 325; (c) A. Butler, *Curr. Opin. Chem., Biol.* 1998, **2**, 279-285; (d) K. E. Liu, A. M. Valentine, D. Qiu, D. E. Edmondson, E. H. Appelman, T. G. Spiro and S. J. Lippard, *J. Am. Chem. Soc.*, 1995, **117**, 4997-4998.

2 (a) R. K. Narla, Y. Dong, O. J. D'Cruz, C. Navara and F. M. Uckun, *Clin. Cancer Res.,* 2000, **6**, 1546-1556; (b) P. P. Hazari, A. K. Pandey, S. Chaturvedi, A. K. Tiwari, S. Chandna, B. S. Dwarakanath and A. K. Mishra, *Chem. Biol. Drug Des.*, 2012, **79**, 223-234.

3 (a) T.L. Fernández, E.T. Souza, L.C. Visentin, J.V. Santos, A.S. Mangrich, R.B. Faria, O.A.C. Antunes and M. Scarpellini, *J. Inorg. Biochem.*, 2009, **103**, 474-479; (b) D. Rehder, G. Santoni, G.M. Licini, C. Schulzke and B. Meier, *Coord. Chem. Rev.*, 2003, **237**, 53-57**;** (c) R.L. Robson, R.R. Eady, T.H. Richardson, R.W. Miller, M. Hawkins and J.R. Postgate, *Nature*, 1986, **322**, 388-390.

4 T. Ueki, T. Adachi, S. Kawano, M. Aoshima, N. Yamaguchi, K. Kanamori and H. Michibata, *Biochim. Biophys. Acta,* 2003,**1626**, 43-50.

5 (a) Y. Shechter, S. J. D. Karlish, *Nature,* 1980, **284**, 556-558; (b) A. Levina and P.A. Lay, *Dalton Trans.*, 2011, **40**, 11675–11686; (c) Y. Shechter, *Diabetes,* 1990, **39**, 1-5.

6 (a) H. John, V. McNeill, G. Yuen, H. R. Hoveyda and C. Orvig, *J. Med. Chem.,* 1992, **35**, 1489-1491; (b) D. Gambino, *Coord. Chem. Rev.*, 2011, **255**, 2193–2220.

7 H. Vilter, *Phytochem.***,** 23, **1984**, 1387–1390.

8 (a) A.G.J. Ligtenbarg, R. Hage and B.L. Feringa, *Coord. Chem. Rev.*, 2003, **237**, 89–101; (b) D. Rehder, G. Santoni, G.M. Licini, C. Schulzke and B. Meier, *Coord. Chem. Rev.*, 2003, **237**, 53-63; (c) V. Kraehmer and D. Rehder, *Dalton Trans.*, 2012, **41**, 5225-5234; (d) A. Butler, *Bioinorganic Catalysis,* 1992, 425-445.

9 (a) T. K. Si, S. S. Paul, M. G. B. Drew and K. K. Mukherjea, *Dalton Trans.*, 2012, **41**, 5805–5815; (b) S. Patra, S. Chatterjee, T. K. Si and K. K. Mukherjea, *Dalton Trans.*, 2013, **42**, 13425–13435.

10 (a) S. Rayati, N. Sadeghzadeh and H. R. Khavasi, *Inorg. Chem. Commun.,* 2007**,** **10**, 1545-1548; (b) H. S. Soedjak, J. V. Walker and A. Butler, *Biochemistry,* 1995, **34**, 12689-12696; (c) B.B. Gangadhar, S.B. Prema and S.A. Patil, *J. Enzyme Inhib. Med. Chem.*,2009, **24**, 381–394.

11 U. Saha, T.K. Si, P.K. Nandi and K.K. Mukherjea, *Inorg. Chem. Commun.*, 2013, **38**, 43–46.

12 (a) M. Sam, J.H. Hwang, G. Chanfreau and M.M. Abu-Omar*, Inorg. Chem.*, 2004, **43**, 8447–8455; (b) P.K. Sasmal, S. Saha, R. Majumdar, S. De, R.R. Dighe, A.R. Chakravarty, DaltonTrans. 39 (2010) 2147–2158.

13 D. R. Tatiana, S. Giampiero, P. Maurizio, T. Saison-Behmoaras, B. Alexandre and B. Cacciari, *Curr. Med. Chem.*, 2005, **12***,* 71-88.

14 (a) G. Verquin, G. Fontaine, M. Bria, E. Zhilinskaya, E. Abi-Aad, A. Aboukaïs, B. Baldeyrou, C. Bailly and J. L. Bernier, *J. Biol. Inorg. Chem.*, 2004, **9**, 345-353; (b) L.G. Naso, E.G. Ferrer, N. Butenko, I. Cavaco, L. Lezama, T. Rojo, S.B. Etcheverry and P.A.M. Williams, *J. Biol. Inorg. Chem.*,2011, **16**, 653–668.

15 (a) P. Nagababu, J. Naveena, L. Latha and S. Satyanarayana, *Chemistry & Biodiversity*, 2006, **3**, 1219-1228.

16 (a) P. Rây, A. K. Mukherjee, *J. Indian. Chem. Soc.,* 1950, **27**, 707; (b) A. K. Mukherjee, P. Rây, *J. Indian. Chem. Soc.,* 1955, **32**, 505-510; (c) G. J. Colpas, B. J. Hamstra, J. W. Kampf and V. L. Pecoraro, *J. Am. Chem. Soc.,* 1994, **116**, 3627-3628; (d) L. J. Theriot, G. O. Carlisle and H. J. Hu, *J. Inorg. Nucl. Chem.,* 1969, **31**, 3303-3308.

17 (a) K. Nakajima, M. Kojima,; K. Toriumi, k. Saito and K. Fujita, *J. Bull Chem. Soc. Jpn.,* 1989, **62**, 760-767; (b) J. C. Pessoa, I. Cavaco, I. Correia, D. Costa, R. T. Henriques and R. D. Gillard, *Inorg. Chim. Acta*., 2000, **305**, 7-13; (c) M. Kirihara, *Coord. Chem. Rev*., 2011, **255**, 2281–2302: (c) H.-Y. Zhao, Y.-H. Xing, Y.-Z. Cao, Z.-P. Li, D.-M. Wei, X.-Q. Zeng and M.-F. Ge, *J. Mol. Struct*., 2009, **938,** 54-64.

18 G. H. Jeffery, J. Bassett, J. Mendham and R. C. D. Addison, *Vogel's Text Book of Quantitative Chemical Analysis*, Wesley Longman Limited, UK, 1989, 5th edn.

19 R.G. Parr and W. Yang, *Density Functional Theory of Atoms and Molecules*, Oxford University Press, Oxford (1989).

20 (a) V. Barone and M. Cossi, *J. Phys.Chem. A*, 1998, **102**, 1995-2001; (b) M. Cossi and V. Barone, *J. Chem. Phys*., 2011, **115**, 4708-4717; (c) M. Cossi, N. Rega, G. Scalmani and V. Barone, *J. Comp. Chem*., 2003, **24**, 669-681.

21 A.D. Becke, *J. Chem. Phys*., 1993, **98**, 5648-5652.

22 C. Lee, W. Yang and R.G. Parr, *Phys. Rev. B*, 1998, **37**, 785-789.

23 M. J. Frisch, G. W. Trucks, H. B. Schlegel, G. E. Scuseria, M. A. Robb, J. R. Cheeseman, G. Scalmani, V. Barone, B. Mennucci, G. A. Petersson, H. Nakatsuji, M. Caricato, X. Li, H. P. Hratchian, A. F. Izmaylov, J. Bloino, G. Zheng, J. L. Sonnenberg, M. Hada, M. Ehara, K. Toyota, R. Fukuda, J. Hasegawa, M. Ishida, T. Nakajima, Y. Honda, O. Kitao, H. Nakai, T. Vreven, J. A. Montgomery Jr., J. E. Peralta, F. Ogliaro, M. Bearpark, J. J. Heyd, E. Brothers, K. N. Kudin, V. N. Staroverov, R. Kobayashi, J. Normand, K. Raghavachari, A. Rendell, J. C. Burant, S. S. Iyengar, J. Tomasi, M. Cossi, N. Rega, J. M. Millam, M. Klene, J. E. Knox, J. B. Cross, V. Bakken, C. Adamo, J. Jaramillo, R. Gomperts, R. E. Stratmann, O. Yazyev, A. J. Austin, R. Cammi, C. Pomelli, J. W. Ochterski, R. L. Martin, K. Morokuma, V. G. Zakrzewski, G. A. Voth, P. Salvador, J. J. Dannenberg, S. Dapprich, A. D. Daniels, Ö. Farkas, J. B. Foresman, J. V. Ortiz, J. Cioslowski and D. J. Fox, *Gaussian 09*, (Revision A.1), Gaussian, Inc., Wallingford, CT, 2009.

24 (a) T. Liu, H.-X. Zhang and B.-H. Xia, *J. Phys. Chem. A*, 2007, **111**, 8724-8730; (b) X. Zhou, H.-X. Zhang, Q.-J. Pan, B.-H. Xia and A.-C.Tang, *J. Phys. Chem. A*, 2005, **109**, 8809-8818; (c) X. Zhou, A.-M. Ren and J.-K. Feng, *J. Organomet. Chem*., 2005, **690**, 338-347. (d) A. Albertino, C. Garino, S. Ghiani, R. Gobetto, C. Nervi, L. Salassa, E. Rosenverg, A. Sharmin, G. Viscardi, R. Buscaino, G. Cross and M. Milanesio, *J. Organomet. Chem*., 2007, **692**, 1377-1391.

25 N. M. O'Boyle, A. L. Tenderholt and K. M. Langner, *J. Comp. Chem*., 2008, **29**, 839-845.

26 E. Verhaeghe, D. Buisson, E. Zekri, C. Leblanc, P. Potin and Y. Ambroise, *Anal. Biochem*., 2008, **379**, 60-65.

27 G.J. Colpas, B.J. Hamstra, J.W. Kampf and V.L. Pecoraro, *J. Am. Chem. Soc*., 1996, **118**, 3469-3478.

28 J. B. Chaires, N. Dattagupta and D. M. Crothers, *Biochemistry*, 1982, **21**, 3933–3940.

29 (a) U.Saha and K. K. Mukherjea, *Int. J. Biol. Macromol*., 2014, **66**, 166–171; (b) M. Selim and K. K. Mukherjea, J. Biomol. Struct. Dyn., 2009, **26**, 561–566; (c) M. Selim, S. R. Chowdhury and K. K. Mukherjea, *Int. J. Biol. Macromol*., 2007, **41**, 579–583.

30 L. Krivosudsky´, P. Schwendt, R. Gyepes and Z. Zak, *Polyhedron,* 2014, **81**, 421–427

31 (a) C. R. Cornman, J. Kampf and V. L. Pecoraro, *Inorg. Chem*., 1992, **31**, 1981-1983.

32 (a) M. R. Maurya and S. Khurana, *Transition Met. Chem*., 2003, **28**, 511-517; (b) P. Raghunathan and B. B. Das, *Chem. Phys. Lett*., 989, **160**, 627-631.

33 E. Froehlich, A. Gupta, J Provencher-Mandeville, E Asselin, J Bariyanga, G. Bérubé and H.-A. Tajmir-Riahi. *DNA & Cell Biology*, 2009 **28**, 31-39.

34 J. K. Barton, A. T. Danishefsky and J. M. Goldberg, J. *Am. Chem. Soc*., 1984, **106**, 2172.

35 T. M. Kelly, A. B. Tossi, D. J. McConnel and T. C. Streakas, *Nucleic Acids Res*., 1985, **13**, 6017-6034.

36 T. Biver, F. Secco, M. R. Tine and M. Venturini, *J. Inorg. Biochem*., 2004, **98**, 33-40.

37 (a) S.R. Chowdhury, M. Selim, S. Chatterjee, S. Igarashi, Y. Yukawa and K.K. Mukherjea, *J. Coord. Chem*., 2012, **65**, 3469–3480;(b) V. Rajendiran, R. Karthik, M. Palaniandavar, H. S. Evans, V.S. Periasamay, M. A. Akbarsha, B. S. Srinag and H. Krishnamurthy, *Inorg. Chem*., 2007, **46**, 8208–8221.

38 S. Satyanarayana, J. C. Dabrowiak and J. B.Chaires, *Biochemistry*, 1992, **31**, 9319-9324.

39 C. V. Kumar and E. H. Asuncion, *J. Am. Chem. Soc*., 1993, **115**, 8547-8553.

